$(CH_3)_2$ results in Table I gives a T_1 at 34 °C of 14.3 s, identical with that in Table II. Even without the temperature correction, the $Os(CO)_4(CH_3)_2$ data in Tables I (low field) and II (high field) agree within 3%—remarkable considering that two different instruments were used.
(19) The various complex effects[20] contributing to the chemical shift tensor are individually largest for heavy metals, so $\Delta\sigma$ and therefore R_1^{CSA} should be largest for carbons bonded to heavy metals.
(20) Evans, J.; Norton, J. R. *Inorg. Chem.* **1974,** *13,* 3042.
(21) The 23.5-kG values at 34 °C were obtained by interpolation from Figure 3. $T_1 = 3.19$ s, $\eta_{CH} = 0.31$, $T_1^{DD} = 20.3$ s, $T_1^{other} = 3.78$ s.
(22) It appears that the requirements for scalar relaxation are less strict than originally suggested: Levy, G. C.; Cargioli, J. D.; Anet, F. A. L. *J. Am. Chem. Soc.* **1973,** *95,* 1527. Even when $T_1^Q(M)$ is much larger than $(\Delta\omega)^{-1}$, the value for which (see ref 14) the maximum scalar contribution is obtained, relaxation by this mechanism can still be important, especially with large J.
(23) The hitherto unappreciated importance of scalar relaxation in determining line widths in ^{11}B spectra has recently been demonstrated: Weiss, R.; Grimes, R. N. *J. Am. Chem. Soc.* **1978,** *100,* 1401.
(24) Mann, B. E. "Nuclear Magnetic Resonance of Nuclei Other Than Protons", Axenrod, T., Webb, G. A., Eds.; Wiley: New York, 1974.
(25) Blunt, J. W.; Stothers, J. B. *J. Magn. Reson.* **1977,** *27,* 515.
(26) Calvert, R. B.; Shapley, J. R. *J. Am. Chem. Soc.* **1977,** *99,* 5225. **1978,** *100,* 7726.
(27) Kuhlmann, K. F.; Grant, D. M. *J. Chem. Phys.* **1971,** *55,* 2998.
(28) If it is assumed that the asymmetric bridging methyl can be characterized by a single effective reorientation correlation time $[\tau_c(CH_3)]^{-1} = [\tau_c(Os_3 \text{ frame motion})]^{-1} + [\tau_c(\text{internal } CH_3 \text{ motion})]^{-1}$, and that $\tau_c(Os_3 \text{ frame motion}) = \tau_c(CH_2)$, then $\Delta G^{\ddagger}$ (internal CH_3 motion) can be estimated as 4 kcal/mol.
(29) (a) Angelici, R. J. "Synthesis and Technique in Inorganic Chemistry", W. B. Saunders: Philadelphia, 1969; p 131. (b) Piper, T. S.; Wilkinson, G. *J Inorg. Nucl. Chem.* **1956,** *3,* 104.
(30) King, R. B. "Organometallic Syntheses", Vol. 1; Academic Press: New York, 1965; p 145.
(31) Tamaki, A.; Kochi, J. K. *J. Organomet. Chem.* **1973,** *61,* 441.
(32) (a) Webb, M. J.; Graham, W. A. G. *J. Organomet. Chem.* **1975,** *93,* 119. (b) Hieber, W.; Braun, G. *Z. Naturforsch.* **1959,** *146,* 132.
(33) George, R. D.; Knox, S. A. R.; Stone, F. G. A. *J. Chem. Soc., Dalton Trans.* **1973,** 972.
(34) Samuel, E.; Rausch, M. D. *J. Am. Chem. Soc.* **1973,** *95,* 6263.
(35) Gillman, H.; Zoellner, E. A.; Selby, W. M. *J. Am. Chem. Soc.* **1933,** *55,* 1252.
(36) Freeman, R.; Hill, H. D. W. *J. Chem. Phys.* **1971,** *54,* 3367.
(37) The 67.8-MHz T_1's were determined at the Yale Regional NMR Facility with the assistance of Peter Demou.
(38) Harris, R. K.; Newman, R. H. *J. Magn. Reson.* **1976,** *24,* 449.
(39) Sass, M.; Ziessow, D. *J. Magn. Reson.* **1977,** *25,* 263.
(40) Small deviations from exponentiality have been observed in the relaxation of the methyl carbons of several linear methylmercury compounds.[5] It appears that highly anisotropic molecular reorientation, such as that present in CH_3HgX, is necessary if such nonexponential effects are to be significant.[41] The compounds studied in the present work are pseudooctahedral or pseudotetrahedral (including CH_3AuPPh_3, which is pseudotetrahedral about phosphorus) and their reorientation is relatively isotropic.
(41) Howarth, O. W., private communication.
(42) Freeman, R.; Hill, H. D. W.; Kaptein, R. *J. Magn. Reson.* **1972,** *7,* 327.
(43) Canet, D. *J. Magn. Reson.* **1976,** *23,* 361.
(44) Kowalewski, J.; Ericsson, A.; Vestin, R. *J. Magn. Reson.* **1978,** *31,* 165.
(45) Farrar, T. C.; Druck, S. J.; Shoup, R. R.; Becker, E. D. *J. Am. Chem. Soc.* **1972,** *94,* 699.
(46) These measurements were kindly performed by Dr. Peter Domaille.

Metal Ion Complexes of α-Amido Acids. 1. Structure and Magnetic Properties of the Nickel and Cobalt Hippurates. Pseudo-One-Dimensional Magnetic Systems

Maurice M. Morelock,[1a] Mary L. Good,*[1b] Louis M. Trefonas,*[1a] David Karraker,*[1c] Lutfollah Maleki,[1a] Helen R. Eichelberger,[1a] Richard Majeste,[1d] and John Dodge[1a]

Contribution from the Department of Chemistry, University of New Orleans, Lakefront, New Orleans, Louisiana 70122, and the Chemistry Division, Savannah River Laboratory, E. I. du Pont de Nemours and Company, Aiken, South Carolina 29801.
Received November 2, 1978

Abstract: The Ni(II) and Co(II) hippurates, $M(hipp)_2(H_2O)_3 \cdot 2H_2O$, have been studied at 298 K by single-crystal X-ray diffraction and UV-visible spectroscopy, and magnetic susceptibility measurements down to 2.2 K have been obtained. The compounds are essentially isostructural and crystallize as linear chains with canted metal octahedra bridged by the oxygen atom of a water molecule. The space group is $C2/c$ with four formula weights per unit cell. The structural properties of the Ni(II) and Co(II) hippurates, respectively, are (1) for Ni, $a = 40.833$ (10) Å, $b = 6.928$ (1) Å, $c = 7.884$ (2) Å, $\beta = 91.92$ (1)°, $R = 0.130$ for 392 reflections; for Co, $a = 40.823$ (7) Å, $b = 6.903$ (1) Å, $c = 7.992$ (2) Å, $\beta = 91.88$ (1), $R = 0.090$ for 715 reflections; (2) the intrachain M-M′ distances (3.942 Å, Ni; 3.966 Å, Co); (3) the interchain M-M* distances along the b axis (6.928 Å, Ni; 6.903 Å, Co); (4) along the a axis, the M-M* distance is about 20 Å in both compounds; (5) the M-O2 (bridging water molecule) distances (2.12 Å, Ni; 2.22 Å, Co); (6) the M-O2-M′ angle (137.2°, Ni; 128.3°, Co); (7) the canting angle, ϕ, made by the canted octahedra with the crystallographic axis (21.4°, Ni; 25.9°, Co). The Ni(II) hippurate complex exhibits a visible spectrum typical of high-spin octahedral Ni(II) complexes; however, the splitting in the visible spectrum of the Co(II) hippurate complex is indicative of the lower site symmetry (C_{2h}) of these compounds. Magnetic susceptibility studies show the Ni(II) hippurate to be an antiferromagnet with $T_c^c \simeq 34$ K and $J = -12.9$ cm^{-1}; the Co(II) hippurate is a metamagnet with $T_c^c \simeq 15$ K and $T_c^b \simeq 3.1$ K. The crystallographic and magnetic susceptibility data indicate that an anisotropic superexchange occurs along the chain (c axis) and that interchain exchange is restricted to dipolar interactions along the b axis. Thus, the nickel and cobalt hippurates constitute pseudo-one-dimensional materials characterized by layers of chains being separated by about 20 Å along the a axis. Since magnetic ordering is not expected between these layers, the nickel and cobalt hippurates represent the first examples of psuedo-one-dimensional magnetic materials in which three-dimensional magnetic ordering is not predicted to occur until $T \rightarrow 0$ K.

Introduction

An earlier communication from our laboratory[2a] reported the initial characterization of a unique cobalt(II) hippurate complex which exhibited a metamagnetic transition at low temperature. The structure was described as a canted, oxygen-bridged linear chain. The structural parameters for this molecule and the analogous nickel(II) complex have now been refined and their respective magnetic properties examined. These molecules represent the first examples of a series of α-amido acid complexes of first-row transition-metal ions

0002-7863/79/1501-4858$01.00/0

which exhibit low dimensional magnetic properties. The hippurate anion and several related carboxylates have been found to form dimers with copper(II)[2b] and polymeric chains with the first-row transition-metal ions iron(II), cobalt(II), and nickel(II). Low-temperature magnetic data for the related manganese(II) complexes indicate that these materials may also be polymeric, exhibiting essentially one-dimensional magnetic character. The details of the iron(II) systems will be presented in a subsequent paper and the structural characterization of the manganese(II) systems is presently being attempted in our laboratory.

Chemists have routinely determined the magnetic properties of inorganic complexes at high temperatures (77 K and above) where normal Curie or Curie-Weiss behavior is generally observed. For paramagnetic materials, the assumption has usually been made that they are magnetically dilute; the calculated susceptibility has been used to determine the magnetic moment (and the number of unpaired electrons) and the presence of low symmetry, and to deduce the Boltzmann distribution between the ground electronic state and thermally accessible excited states. The relatively recent development of cryogenic systems for a variety of physical measurements has provided the incentive for determining magnetic susceptibilities at low temperatures (down to liquid helium temperatures and below) for an ever-increasing number of inorganic materials. At these temperatures, deviations from Curie and Curie-Weiss behavior become common, and new information about the detailed atomic and molecular properties of the systems can be obtained.[3] The deviations from Curie behavior are usually caused by magnetic interactions, both short range and long range. Mathematical models for such interactions have been a long-time interest of theoretical physicists.[4,5] The accumulation of structural and magnetic data for a variety of magnetically nondilute inorganic systems provides the necessary focus for the refinement and ultimate utility of such models. Thus, the synthesis and characterization of new series of magnetically interesting materials become a challenge.

Short-range magnetic interactions arise basically in two ways. Direct metal orbital overlap provides a pathway for spin coupling which results in significantly reduced moments or ultimately in diamagnetic materials; there are many examples of such metal-metal bonding in inorganic complexes.[6-8] When a bridging ligand is present, a second short-range interaction is possible which utilizes the orbitals of the bridging ligand. This mechanism, referred to as superexchange, can result in ordering where spins are aligned parallel (ferromagnetic) or antiparallel (antiferromagnetic). The magnitude of the superexchange interaction decreases as the number of intervening atoms increases and depends critically on the bond distances and angles of the M-X-M pathway.[9-12] For example, it has been observed that in M-X-M systems, where M is Cu(II) or Cr(III), antiferromagnetic coupling is at a maximum with a bridging angle of 180° and decreases as the angle decreases, i.e., spin pairing depends upon nonorthogonality of the orbitals involved in the superexchange pathway. At 97-98° the coupling becomes ferromagnetic with a maximum observed at 90°.[13] The magnitude of the ordering involves interaction of discrete spin quanta and the general quantum mechanical operator can be written explicitly as

$$\mathcal{H} = -2J \sum_{i>j} [aS_i^z S_j^z + b(S_i^x S_j^x + S_i^y S_j^y)] - g\beta \sum_{i=1} HS_i \quad (1)$$

When J is positive, the ordered state is ferromagnetic; a negative J indicates antiferromagnetic ordering. The parameters a and b describe the spin anisotropy of the interaction. The general expression reduces to three special cases: (1) the one-dimensional or Ising model where $a = 1, b = 0$; (2) the planar Heisenberg or XY model where $a = 0, b = 1$; (3) the wholly isotropic or Heisenberg model where $a = b = 1$.

The second part of eq 1 expresses the single ion effects. Although there is no explicit contribution to the exchange interaction through this term, the single ion anisotropy (expressed by g) determines the types of spin exchange that are possible. For example, consider the effect of single ion anisotropy on dipole-dipole spin coupling. For totally isotropic ions in a totally isotropic lattice, the magnetic moment on each ion is directed equally in all directions; since there is no preferred spin orientation, neighboring ions are not expected to affect one another on a dipolar basis until $T \rightarrow 0$. Single ion anisotropy also determines the nature of the superexchange interaction. For totally isotropic ions, only isotropic superexchange is possible, i.e., there can be no dipole-dipole interactions; for anisotropic ions, however, isotropic and anisotropic superexchanges are possible (if the proper crystallographic symmetry exists) and can give rise to two entirely different magnetic phenomena.

Long-range ordering and short-range ordering are often ambiguously discussed since all short-range ordering eventually leads to long-range ordering. The transition from short-range to long-range ordering can be approximated graphically from the magnetic susceptibility data and is observed to occur at some critical temperature, T_c; as a general rule $J \propto kT_c$. T_c is theoretically defined as the temperature at which a three-dimensional magnetic ordering occurs. However, magnetic ordering in each dimension may be observed to occur separately, especially in low-dimensional systems. Therefore, we have chosen to use T_c to represent the critical temperature for magnetic ordering in a particular dimension (e.g., T_c^a is the critical temperature observed experimentally for magnetic ordering along the a axis). It should be pointed out that, although a magnetic phenomenon may not be obvious above its critical temperature, ordering associated with this phenomenon occurs well above T_c. Consequently, it becomes absolutely essential to determine the ground-state magnetic spin structure since all other magnetic phenomena occurring at higher temperatures will certainly be affected by ordering of the magnetic ground state.

An example which has been intensively studied is $CsCoCl_3 \cdot 2H_2O$, which is an Ising canted linear chain with a chloride bridging ligand and a Co-Cl-Co angle of 128°.[14,15] The cobalt ion is octahedrally surrounded by four chloride ions and two water molecules, and the intrachain interaction is antiferromagnetic with the easy or preferred axis perpendicular to the chain. The intrachain spin canting produces a net moment along the chain via an anisotropic superexchange mechanism, generally referred to as D-M or the Dzyaloshimsky-Moriya interaction.[16,17] The interchain interaction between nearest-neighbor chains occurs through a hydrogen-bonded superexchange pathway and is ferromagnetic; consequently a layer of nearest-neighbor chains comprises a magnetic sublattice in which all the D-M moments are aligned parallel. A three-dimensional magnetic ordering occurs below 3.38 K by aligning the moments of alternating sublattices antiparallel. As the temperature is lowered in the presence of a constant field, the magnetization of each sublattice increases, strengthening the long-range antiferromagnetic interaction between sublattices as is experimentally indicated by a decrease in the susceptibility. The lower the temperature, the larger the field required to induce the ferromagnetic transition; i.e., the system is a metamagnet.[18] Another system exhibiting similar magnetic properties is the ligand-bridged $Ni(NO_3)_2 \cdot H_2O$.[19] Several linear chain systems having ligand bridges and exhibiting metamagnet properties have been investigated, notably $MCl_2 \cdot 2H_2O$ and $M(pyr)_2Cl_2$ where M is Fe(II), Co(II), and Ni(II).[18] The Co(II) and Ni(II) hydrated

hippurate chain systems reported herein represent the first examples of a new set of such canted, linear chain systems where the bridging atom is the oxygen of a water molecule and the structural network is held together by intra- and interchain hydrogen bonding. Qualitative correlations between structural and magnetic parameters are presented, and the application of simple magnetic models is explored. The similarities and differences of these complex ligand systems as compared to the well-studied halide materials are delineated.

Experimental Section

Synthetic Procedures. The $M(hipp)_2(H_2O)_3 \cdot 2H_2O$ (M = Ni, Co) complexes were prepared as described by Eichelberger.[20] Stoichiometric amounts of $M(ClO_4)_2 \cdot 6H_2O$ and the sodium salt of hippuric acid (mole ratio of 1:2) were mixed in a 1:1 ethanol/water solution. Needle and plate-like crystals formed from high and low concentrations of the reactants, respectively. The crystals were filtered and air dried. Recrystallization was accomplished by first dissolving the dried crystals in water and diluting until a pale-colored solution was formed. The resulting solution was transferred to a small beaker and placed in a closed apparatus containing ethanol as described by Brown and Trefonas.[21] Plate-like crystals began to form within 1 week. As the metal hippurate solution became colorless, the solvent was decanted and a fresh dilute solution added. This process was continued for about 3 months before crystals of a quality even minimally suitable for an X-ray diffraction study were obtained. Elemental analysis, including careful determination of total water by thermal gravimetric techniques, provided the overall stoichiometry of the complexes. Representative results follow.

Anal. Calcd for $Co(C_6H_5CONHCH_2CO_2)_2 \cdot 5H_2O$: C, 42.78; H, 5.19; Co, 11.66; H_2O, 17.8. Found: C, 42.80; H, 5.11; Co, 11.93; H_2O, 18.2. Calcd for $Ni(C_6H_5CONHCH_2CO_2)_2 \cdot 5H_2O$: C, 42.80; H, 5.19; Ni, 11.62; H_2O, 17.87. Found: C, 42.36; H, 5.15; Ni, 11.59; H_2O, 17.3.

It should be pointed out that these complexes have a different stoichiometry from the Co(II) and Ni(II) hippurate complexes reported by Marcotrigiano and Pellacani.[22] These authors used different stoichiometric ratios of starting materials and obtained materials of empirical formula $M(hipp)_2 \cdot 6H_2O$ where M = Co(II) or Ni(II).

Physical Methods. Visible absorption spectra were obtained on a Cary 17 recording spectrophotometer. Samples were prepared as Nujol mulls and mounted on Whatman no. 1 filter paper. Nujol-soaked filter paper was used as a reference. Each absorption band was fitted by hand to the equation $y = ae^{-(b-x)^2}$ where a and b are the absorbance and frequency, respectively, at peak maximum. Two or three peaks were thus assigned until the summation of the Gaussian set of peaks gave a close fit to the observed experimental curve. Since a unique fit was not possible, the assignment was made in terms of the major Gaussian band nearest to λ_{max} of the experimental curve.

EPR spectra of the powdered samples were recorded on a Varian E-3 X-band spectrometer. Line positions were determined relative to the external field strength. Polycrystalline diphenyldipicrylhydrazil (DPPH, $g = 2.0036$) was used as a g-value standard.

The high-temperature magnetic susceptibility data were determined on powdered, polycrystalline samples using a Cahn 7600 Faraday magnetic balance equipped with a Cahn DTL electrobalance. Low-temperature magnetic data (2.2–80 K) were determined for the same samples using a Forner-type vibrating-sample magnetometer (manufactured by Princeton Applied Research Corp.) operated in the field of a 12-in. electromagnet. A germanium resistance thermometer mounted directly behind the sample measured the temperature. All systems were calibrated with $Hg[Co(NCS)_4]$ as a standard.

Collection and Reduction of X-ray Data. X-ray diffraction data were obtained using a Norelco SRG 5000 X-ray generator with a Cu Kα source and collected on the Norelco IC 200 read-out system. The resulting powder patterns indicated that the Ni(II) and Co(II) hippurate complexes were very nearly isomorphous.

Single crystals of the two complexes having no dimension greater than 0.25 mm were selected for preliminary single-crystal diffraction studies using a General Electric XRD-5 diffractometer. In the case of the Co(II) complex, systematic extinctions (hkl, $h + k = 2n + 1$; $h0l$, $l = 2n$) indicated that the space group was either Cc or $C2/c$. Lattice constants were determined by a least-squares fit of 15 carefully measured values of the copper Kα_1 and Kα_2 doublet for reflections with $2\theta > 67°$ under fine conditions (1° takeoff angle and 0.05° slit). The resultant lattice constants and their estimated deviations are $a = 40.823$ (7) Å, $b = 6.903$ (1) Å, $c = 7.992$ (2) Å, and $\beta = 91.88$ (1)°. The calculated density of 1.49 g/cm^3 for four molecules per unit cell agrees with the experimental density of 1.47 ± 0.02 g/cm^3 measured by flotation techniques.

Three-dimensional intensity data were collected on a General Electric XRD-490 fully automated diffractometer using balanced nickel and cobalt filters with copper Kα radiation. A total of 1005 independent reflections were measured to a 2θ maximum of 100°. Of these, 715 reflections (71%) were considered statistically significant by the criterion

$$[I_{Ni} - 2\sigma(I_{Ni})] - [I_{Co} - 2\sigma(I_{Co})] > T$$

where $T = 75$ and the σ's were based entirely on counting statistics. The intensities were corrected for Kα_1–Kα_2 splitting as a function of 2θ and for absorption as a function of φ (linear absorption coefficient = 6.8 cm^{-1} and maximum difference of 13.2% over the entire range). Lorentz-polarization corrections were made and the intensities reduced to structure amplitudes in the usual manner.

A preliminary study of the extinctions and cell parameters for the Ni(II) complex showed it to be isomorphous with the cobalt complex. Lattice constants were carefully determined by a least-squares fit of 15 values of the copper Kα_1 and Kα_2 doublet for reflections with $2\theta > 55°$. The resultant lattice constants are $a = 40.833$ (10) Å, $b = 6.928$ (8) Å, $c = 7.884$ (2) Å, and $\beta = 91.92$ (1)°.

A total of 562 independent reflections were measured to a 2θ maximum of 70°, with 392 reflections (70%) of these considered statistically significant by the criterion given above with $T = 25$. These values were also corrected for Lorentz-polarization effects, Kα_1–Kα_2 splitting, and absorption. The maximum experimental absorption difference was 35.5%, despite the lower linear absorption coefficient of 17.3 cm^{-1} (as compared to the cobalt case) because of the more plate-like shape of the nickel hippurate crystals.

Determination and Refinement of Structures. The three-dimensional Patterson function for the cobalt structure showed the four heavy atoms occupying apparent centers of symmetry as indicated by space group $C2/c$. Further refinements in both space groups proved this to be correct. A Fourier map was phased based on the location of the cobalt atoms, and this was used to obtain the remaining nonhydrogen atom coordinates. The resulting structure was refined using block-diagonal least squares with isotropic temperature factors to a value of $R = 0.116$.[23] The final refinements with all atoms anisotropic, anomalous dispersion corrections for the cobalt atoms, and $1/\sigma^2$ weights terminated with a final value of $R = 0.090$.

Refinement was initiated for the nickel structure using the previously refined atom parameters obtained from the cobalt structure as starting coordinates and assigning initial isotropic temperature factors of 4.0 Å^2 to each atom. The structure refined readily, but because of the limited data set only the nickel was assigned anisotropic temperature factors in further refinements. The final refinements using anomalous dispersion corrections for the nickel atoms and $1/\sigma^2$ weights resulted in a value of $R = 0.130$.

Results and Discussion

Structures. The final least-squares coordinates and temperature factors with estimated standard deviations for each parameter are summarized for the cobalt hippurate in Table I and for the nickel hippurate in Table II. The estimated standard deviations (esd's) are less than 0.01 Å for Co–O distances and 0.4° for O–Co–O angles. The esd's for the nickel are less than 0.02 Å for Ni–O distances and 0.8° for O–Ni–O angles. However, since both the cobalt and nickel atoms occupy special positions in the cell, the measurements of the Co–Co separation (3.996 Å) and the Ni–Ni separation (3.942 Å) have the same accuracy as that obtained in the unit cell measurements and consequently each have esd values of 0.001 Å.

Figure 1 shows the geometry about the heavy atoms in each of the structures. The heavy atoms lie on centers of symmetry, each bonded to two hippurate molecules and two water molecules in the central plane. These planes are linked to each other in an infinite chain by a bridging water molecule. The metal–oxygen bonds in the bridge are longer than the other metal–oxygen distances (2.22 Å as compared to 2.06 and 2.04 Å in the cobalt structure and 2.12 Å as compared to 2.07 and 2.00

Table I. Fractional Coordinates and Thermal Parameters[a]

atom	X	Y	Z	β_{11}	β_{22}	β_{33}	β_{12}	β_{13}	β_{23}
Co	0.5000(0)	0.5000(0)	0.5000(0)	5(0)	134(12)	34(7)	1(2)	−1(1)	4(10)
O-1	0.4633(2)	0.3223(18)	0.5754(12)	4(1)	232(42)	77(23)	−6(6)	4(4	−11(26)
O-2	0.5000(0)	0.6402(22)	0.7500(0)	9(2)	83(51)	9(28)	0(0)	−9(5)	0(0)
O-3	0.4423(3)	0.2310(18)	0.3278(12)	10(1)	220(44)	58(22)	−11(6)	−4(4)	−24(26)
O-4	0.3669(3)	0.3736(19)	0.4212(16)	13(1)	132(42)	250(33)	2(7)	−27(6)	14(32)
O-5	0.4650(3)	0.6930(17)	0.4115(12)	8(1)	114(35)	51(21)	3(5)	−11(4)	10(24)
O-6	0.4024(3)	0.3266(17)	0.0417(13)	7(1)	117(37)	130(25)	−2(6)	−1(4)	2(26)
N-1	0.3870(3)	0.0800(20)	0.4798(15)	5(1)	104(43)	75(28)	5(6)	0(4)	62(27)
C-1	0.4405(4)	0.2360(26)	0.4875(20)	7(2)	78(57)	138(40)	3(9)	−6(6)	12(39)
C-2	0.4136(3)	0.1544(26)	0.5856(18)	1(1)	166(61)	100(35)	−12(7)	0(5)	4(38)
C-3	0.3649(4)	0.1963(27)	0.4075(20)	9(2)	142(59)	104(38)	−16(9)	2(6)	−32(41)
C-4	0.3365(5)	0.1139(28)	0.3141(20)	9(2)	197(65)	72(38)	−2(9)	0(6)	2(40)
C-5	0.3126(5)	0.2406(29)	0.2391(23)	9(2)	225(76)	204(48)	3(10)	−5(8)	49(49)
C-6	0.2826(4)	0.1690(35)	0.1607(23)	6(2)	476(96)	207(49)	5(12)	−7(7)	−49(61)
C-7	0.2775(5)	−0.0277(36)	0.1406(22)	14(2)	416(95)	137(45)	18(14)	−3(8)	3(58)
C-8	0.3010(5)	−0.1499(32)	0.2026(23)	8(2)	329(84)	196(48)	−19(11)	1(7)	−60(53)
C-9	0.3307(5)	−0.0809(30)	0.2941(22)	11(2)	223(71)	136(44)	−4(10)	5(7)	46(45)

[a] Anisotropic temperature factors of the form $\exp[-(\beta_{11}h^2 + \beta_{22}k^2 + \beta_{33}l^2 + 2\beta_{12}hk + 2\beta_{13}hl + 2\beta_{23}kl)]$. Anisotropic thermal parameters $\times 10^4$, estimated standard deviations in parentheses refer to last decimal place.

Table II. Fractional Coordinates and Thermal Parameters[a]

atom	X	Y	Z	β_{11}	β_{22}	β_{33}	β_{12}	β_{13}	β_{23}
Ni	0.5000(0)	0.5000(0)	0.5000(0)	11(1)	207(31)	7(16)	−4(5)	7(3)	−27(21)
O-1	0.4641(4)	0.3204(33)	0.5638(23)	3.7(5)					
O-2	0.5000(0)	0.6114(47)	0.7500(0)	3.8(8)					
O-3	0.4426(4)	0.2366(33)	0.3255(23)	3.8(5)					
O-4	0.3678(6)	0.3745(42)	0.4188(30)	8.1(8)					
O-5	0.4655(4)	0.7008(34)	0.4163(23)	4.2(6)					
O-6	0.4030(5)	0.3287(35)	0.0293(25)	4.9(6)					
N-1	0.3888(6)	0.0762(44)	0.4756(32)	5.1(8)					
C-1	0.4401(7)	0.2435(52)	0.4913(35)	3.2(8)					
C-2	0.4145(7)	0.1568(53)	0.5838(37)	4.4(9)					
C-3	0.3658(8)	0.1880(56)	0.4130(39)	5.4(10)					
C-4	0.3377(9)	0.1145(65)	0.3173(44)	7.2(12)					
C-5	0.3109(9)	0.2256(70)	0.2382(49)	8.5(13)					
C-6	0.2794(10)	0.1815(72)	0.1589(51)	9.8(14)					
C-7	0.2783(8)	−0.0182(70)	0.1410(45)	7.4(11)					
C-8	0.3009(10)	−0.1626(71)	0.2034(51)	9.0(13)					
C-9	0.3315(9)	−0.0939(76)	0.3102(48)	8.5(13)					

[a] Anisotropic temperature factors of the form $\exp[-(\beta_{11}h^2 + \beta_{22}k^2 + \beta_{33}l^2 + 2\beta_{12}hk + 2\beta_{13}hl + 2\beta_{23}kl)]$. Isotropic temperature factors of the form $\exp[-(\beta_{11}(\sin^2\theta)/\lambda^2]$. Thermal parameters $\times 10^4$, estimated standard deviations in parentheses refer to last decimal place.

Å in the nickel structure) forming a tetragonally distorted octahedron. This distortion is much more pronounced in the cobalt structure than in the nickel. Also of note is the longer Co–Co separation of 3.996 Å as compared to the Ni–Ni separation of 3.942 Å across the water bridge.

The backbone of the structure extends in an infinite chain along the *c* cell axis. The hippurate molecules are bonded to the cobalt through the carboxyl oxygen atoms as has been previously observed in the case of copper hippurate.[2,24,25] Figure 2 shows the hippurate groups fanning out from the backbone like alternating rungs of a ladder. The metal-bonded and lattice water molecules appear to be involved in an inter- and intrachain H-bonding network (see Figures 2 and 3). The bond angles involving the oxygen atoms of these water molecules are taken to be representative of the H–O–H angle with the H atoms lying between oxygen atoms. For example, the lattice water molecule forms angles, O5–O6–O4, of 113.4 and 117.0° for the cobalt and nickel analogues, respectively. The lattice water molecule thus serves to anchor the bulky hippurate molecule in place and is also involved in the interchain H bonding. As can be seen from Figure 3, interchain H bonding serves to hold chains together along the *b* axis forming a layer of chains in the *bc* plane. Figure 4 shows a unit cell looking down the *z* axis. The only interaction between *bc* planes appears to be a van der Waals attraction along the *a* axis between the benzene rings of one *bc* plane and the next. This type of bonding along the *a* axis is so weak that the crystals grow as thin plates and there is a tendency for *bc* planes to slide along the *c* axis when pressure is applied.

UV–Visible Spectra. The UV–visible spectrum of $Ni(Hipp)_2(H_2O)_3 \cdot 2H_2O$ is typical of that exhibited by Ni(II) high-spin complexes (see Figure 5). Although the site symmetry as discussed above is $\sim C_{2h}$, the observed deviations from octahedral symmetry are not expected to greatly affect the electronic spectra of high-spin nickel(II) complexes. Thus, the observed bands can be assigned on the basis of O_h symmetry as follows: 8.5×10^3 cm^{-1}, $^3T_{2g}(F) \leftarrow {}^3A_{2g}(F)$; 13.8×10^3 cm^{-1} (sh), $^1E_g(D) \leftarrow {}^3A_{2g}(F)$; 25.8×10^3 cm^{-1}, $^3T_{1g}(P) \leftarrow {}^3A_{2g}(F)$. Another alternative is to consider D_{4h} symmetry with tetragonal distortion along the H_2O bridge axis. The observed bands are then assigned: 8.5×10^3 cm^{-1}, $^3B_{2g}$, $^3E_g(F) \leftarrow {}^3B_{1g}(F)$; 15.3×10^3 cm^{-1}, $^3A_{2g}(F) \leftarrow {}^3B_{1g}(F)$; 13.8×10^3 cm^{-1} (sh), $^3E_g(F) \leftarrow {}^3B_{1g}(F)$; 25.8×10^3 cm^{-1}, $^3A_{2g}$, $^3E_g(P) \leftarrow {}^3B_{1g}(F)$. Assignments to lower symmetries are not feasible owing to the lack of any additional band splitting. The spectrum was considered to be characteristic of essentially octahedral symmetry with crystal field parameters of $Dq = 975$ cm^{-1} and $B = 855$ cm^{-1} (79.2% free ion value).

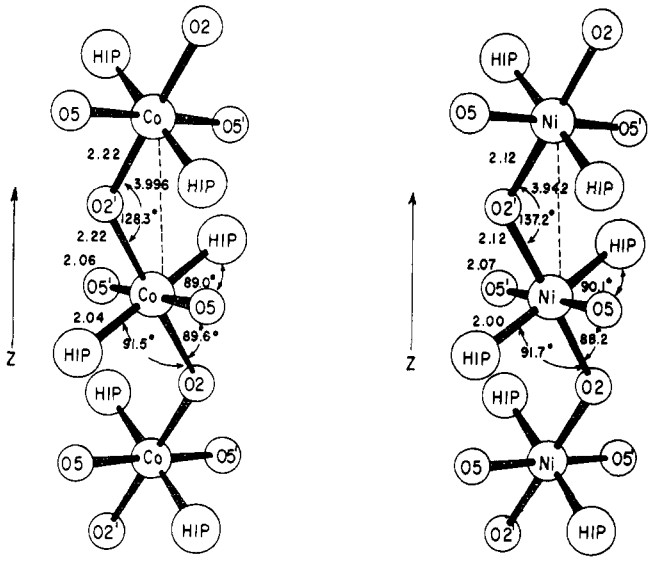

Figure 1. Projection view of the site symmetry about the Co(II) and Ni(II) ions.

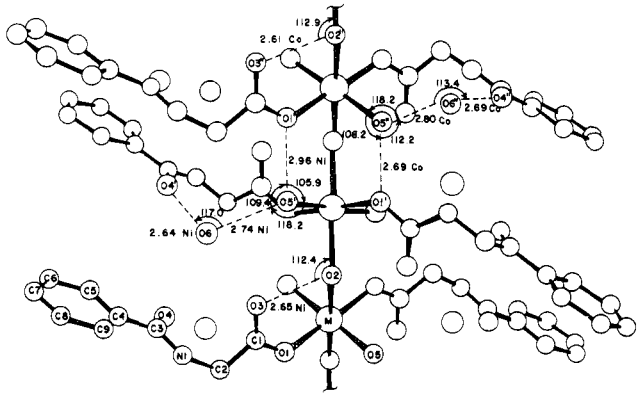

Figure 2. The $M(Hipp)_2(H_2O)_3 \cdot 2H_2O$ molecule, where M = Ni(II), Co(II). Hydrogen bonding involving the lattice water molecules is shown as dashed lines.

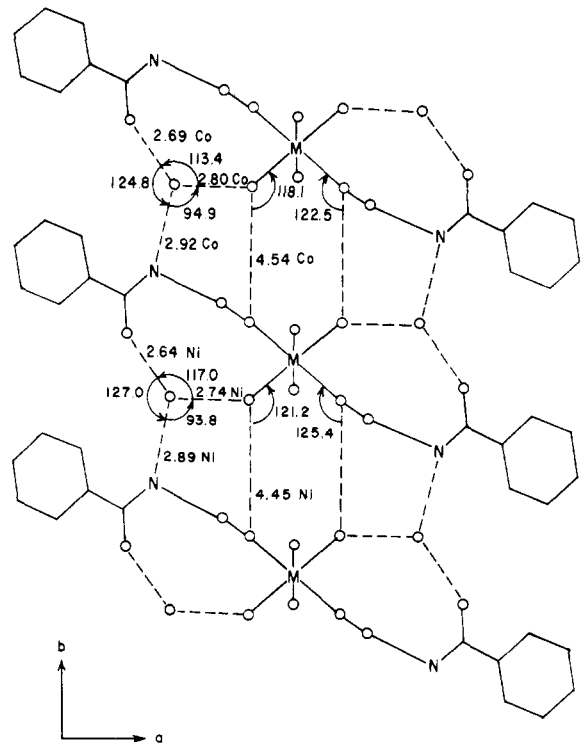

Figure 3. Proposed interchain hydrogen bonding along the *b* axis for the Ni(II) and Co(II) hippurates.

In contrast, a multiplicity of bands in the UV-visible spectrum of $Co(Hipp)_2(H_2O)_3 \cdot 2H_2O$ is indicative of significant deviations from simple octahedral symmetry (see Figure 5). The spectrum is very similar to that exhibited by $CoCl_2 \cdot 6H_2O$[26] in which the site symmetry is also C_{2h}. Therefore, analogous assignments were made for $Co(Hipp)_2(H_2O)_3 \cdot 2H_2O$ complex. The ground-state term in O_h symmetry is $^4T_{1g}(F)$; as the symmetry is lowered, the $^4T_{1g}$ reducible representation correlates with $^4A_g(d_{xy})$ and $^2{}^4B_g(d_{xz},d_{yz})$ in C_{2h} symmetry. Since tetragonal distortion is apparent along the bridging water molecule axis, ^4B_g was assigned as the ground state. The observed bands are then assigned in C_{2h} symmetry as follows: 8.3×10^3 cm^{-1}, ^4B_g, ^4A_g, $^4B_g(F) \leftarrow {}^4B_g(F)$; 19.2 $\times 10^3$ cm^{-1} (accidental degeneracy), $^4A_g(F)$, $^4A_g(P) \leftarrow {}^4B_g(F)$; 20.5×10^3 cm^{-1}, $^4A_g(P) \leftarrow {}^4B_g(F)$; 22.4×10^3 cm^{-1}, $^4B_g(P) \leftarrow {}^4B_g(F)$. Dq and B were approximated using O_h site symmetry; Dq = 1090 cm^{-1} and B = 901 cm^{-1} (80.4% free ion value). These crystal field parameters are very similar to the results obtained for the Ni(II) hippurate complex as outlined above.

Magnetic Susceptibilities. Since the nickel and cobalt hippurates are structurally similar, their magnetic behavior would be expected to be similar in that primary magnetic interactions arise from structural and symmetry considerations, while single ion differences are usually manifested as perturbations on the entire magnetic system. Thus, our analysis of the powder susceptibility data relies heavily on the respective crystallographic parameters for establishing an appropriate magnetic model. The intrachain M-M′ distances (3.942 Å, Ni; 3.966 Å, Co) are much larger than the sums of the metal ion covalent radii (2.30 Å, Ni; 2.32 Å, Co) and direct exchange as a result of metal-metal orbital overlap would be expected to be negligible. However, superexchange along the *c* axis should be possible through the oxygen atom, O2, of the bridging water molecule, although H_2O has not previously been reported to mediate such a pathway. If the bonding of the M-O2-M′ is similar to that observed in the analogous copper(II) and chromium(III) halide, hydroxide, and sulfide systems (see Introduction), then the sign and relative magnitude of the superexchange along the crystallographic *c* axis, J_c^S, can be empirically predicted from two structural features: (1) the M-O2-M′ angle (Θ = 137.2°, Ni; 128.3°, Co); (2) the M-O2 bond distance (2.12 Å, Ni; 2.22 Å, Co). Since Θ for both compounds is much greater than 100°, the superexchange should be antiferromagnetic with the sign of J_c^S negative. Θ(Ni) is significantly larger than Θ(Co) indicating that $|J_c^S|$ should be larger in the nickel system. The shorter M-O2 bond distance in the nickel would also lead to a prediction of a larger $|J_c^S|$ for nickel since superexchange involves spin pairing throughout the superexchange pathway, i.e., increasing orbital overlap (decreasing bond distance) increases $|J^S|$.

The magnetic susceptibility data for the nickel and cobalt hippurates are shown in Figures 6 and 7, respectively. The nickel system deviates from Curie-Weiss behavior below 60 K and exhibits a broad maximum at about 34 K indicating the predicted antiferromagnetic transition along the chain; the cobalt system deviates from Curie-Weiss behavior below 40 K and also displays a broad antiferromagnetic transition with $T_c^c \simeq 15$ K. Since this antiferromagnetic transition is present in both systems and is the first spin exchange to become evident as kT energy is removed from the system, it is considered to be the primary intrachain interaction arising through a superexchange mechanism. If the exchange is limited to only one

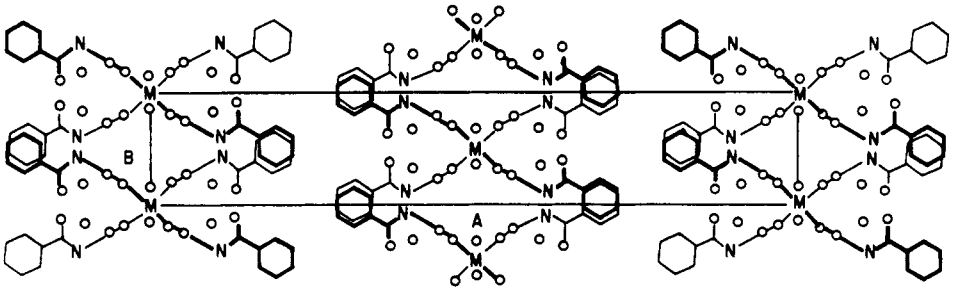

Figure 4. The unit cell of the Ni(II) and Co(II) hippurates as viewed down the c axis. The bold lines are used to illustrate that only two hippurate molecules are bonded to each metal and that they are trans to one another. Although the hippurate configuration is staggered along the c axis, all metals in the same ab plane have the same hippurate configuration.

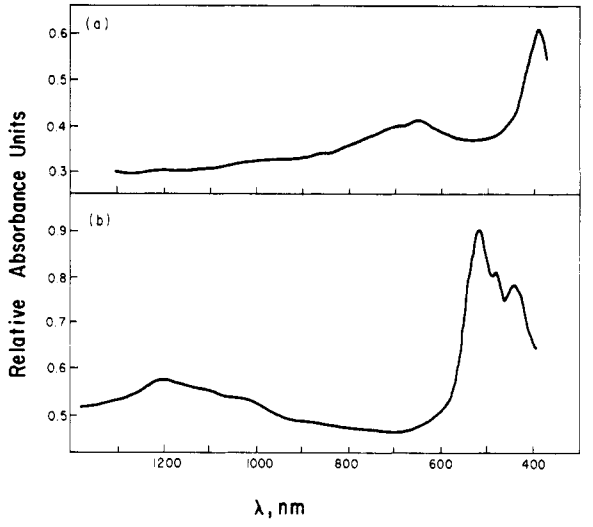

Figure 5. Spectra of $M(Hipp)_2(H_2O)_3 \cdot 2H_2O$: (a) M = Ni(II); (b) M = Co(II).

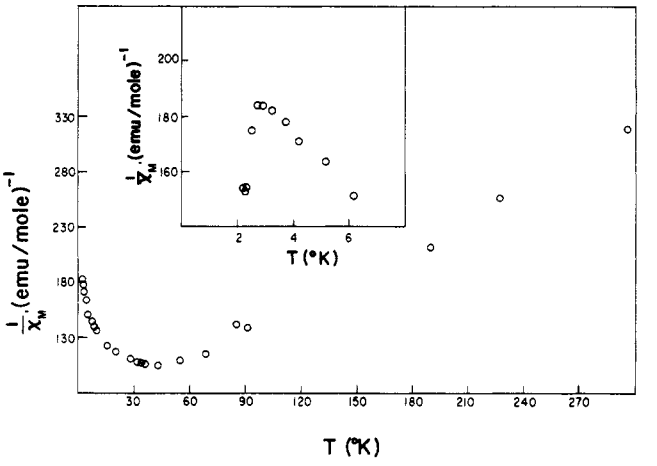

Figure 6. Inverse of the magnetic susceptibility vs. temperature for a powdered sample of $Ni(Hipp)_2(H_2O)_3 \cdot 2H_2O$. Inset shows a sharp increase in the susceptibility below 2.8 K.

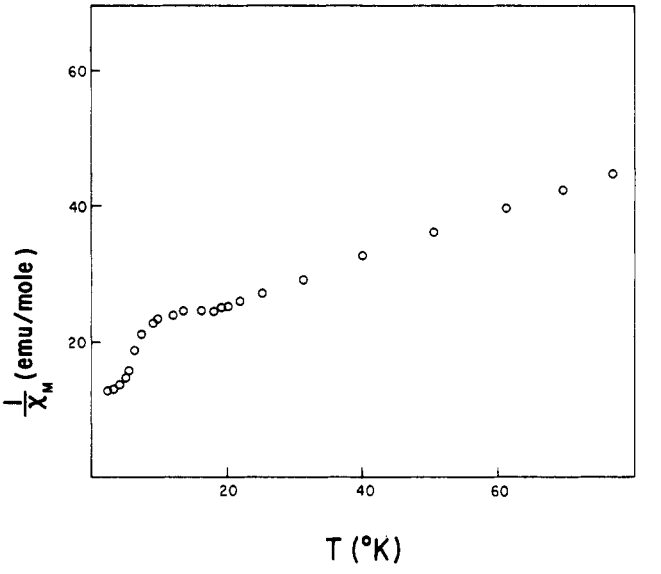

Figure 7. Inverse of the magnetic susceptibility vs. temperature for a powdered sample of $Co(Hipp)_2(H_2O)_3 \cdot 2H_2O$.

direction, the Hamiltonian from eq 1 reduces to

$$\mathcal{H} = -2J \sum_{i=1}^{N} S_i S_{i-1} - g\beta \sum_{i=0}^{N} HS_i \qquad (2)$$

for linear chain systems with isotropic ions. In the classical limit of infinite spin, Fisher showed that using this Hamiltonian the problem becomes exactly solvable.[27] The relationship thus obtained for the susceptibility may be scaled for the finite spin of each metal ion and for N number of ions, or spins, per chain to obtain

$$\chi = \frac{Ng^2\beta^2 S(S+1)}{3kT} \frac{1+U}{1-U} \qquad (3)$$

where S is the spin quantum number, β is the Bohr magneton, k is Boltzmann's constant, g is the electronic splitting factor, and T is temperature. For isotropic Heisenberg coupling in one dimension, U is given by the following expression:

$$U = \coth [2JS(S+1)/kT] - kT/2JS(S+1) \qquad (4)$$

The EPR spectra of the nickel system display a broad, unresolved signal at room temperature and 77 K; the effective spin was obtained by equating the experimental Curie constant with the corresponding part of eq 3 and substituting the value of g obtained from the EPR measurement (g = 2.2, Ni).

$$C^{exp} = \frac{Ng^2\beta^2 S_{eff}(S_{eff}+1)}{3k} \qquad (5)$$

A least-squares program fitted the nickel data to eq 3 using S = 0.98 and keeping J/k as the only adjustable parameter. The result is shown as a solid curve corresponding to $J = -12.9$ cm^{-1} in Figure 8. The experimental data fit the theoretical curve quite well at high temperature. As the temperature is lowered below T_c, deviations from theory become increasingly pronounced until about 3 K, where a sharp increase in the susceptibility is observed (see Figure 6).

The sharp increase in the magnetic susceptibility occurs in both compounds and is even more evident in the cobalt system beginning at about 10 K. The phenomenon appears very similar to the X-Y planar superexchange interaction observed in

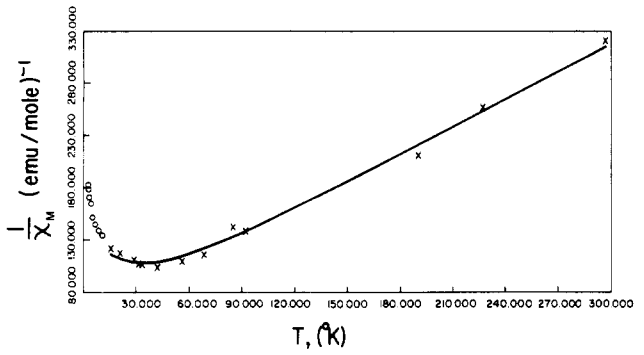

Figure 8. Best fit for the magnetic susceptibility of $Ni(Hipp)_2(H_2O)_3 \cdot 2H_2O$ using Fisher's model for linear chain systems (see text). Open circles show deviations arising from magnetic anisotropy and were not used to obtain best fit.

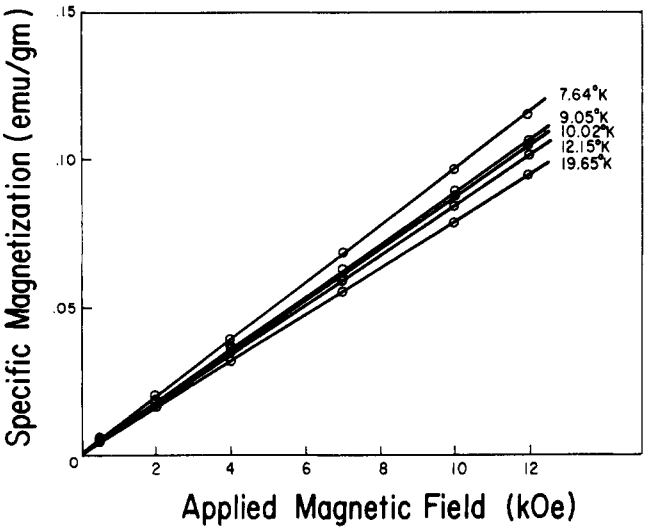

Figure 9. Specific magnetization vs. applied field strength in the 6-20 K temperature range for $Co(Hipp)_2(H_2O)_3 \cdot 2H_2O$.

$CsCoCl_3 \cdot 2H_2O$ where there is an antiferromagnetic superexchange along one axis and a ferromagnetic superexchange of much weaker magnitude along a perpendicular axis.[15] As seen in Figure 3, hydrogen bonding is proposed to occur between chains along the *b* axis and might be viewed as a possible interchain superexchange pathway. One pathway, M-O5-H···O1-M*, is quite analogous to the interchain superexchange pathway proposed for $CsCoCl_3 \cdot 2H_2O$[15] (M-O-H···Cl-M*) in which the exchange is weak and ferromagnetic (J^S = 3.1 cm^{-1}). J^S for this exchange would be expected to be smaller in the nickel and cobalt hippurates (if indeed it does occur) due to the large O5-O1* distance (4.45 Å, Ni; 4.54 Å, Co) as compared to the O-Cl* interchain distance of 3.17 Å in $CsCoCl_2 \cdot 2H_2O$. An even weaker interchain superexchange pathway would be expected through the lattice water molecules. Although the O6-N1* contact distances are much shorter (2.89 Å, Ni; 2.92 Å, Co), the large number of intervening atoms in any superexchange pathway between M and M* quenches the interaction. Furthermore, superexchange along the *a* axis is expected to be virtually nonexistent since there are no plausible superexchange pathways. Based on this structural analysis, $|J_c^S| \gg |J_b^S| > |J_a^S| = 0$. Therefore, superexchange is expected to order significantly in only one dimension, thereby excluding the possibility of *X-Y* planar superexchange.

Interchain interactions along the *a* and *b* axes are expected to arise primarily from dipolar coupling and the magnitude of this type of spin exchange should be proportional to r^{-3}, where

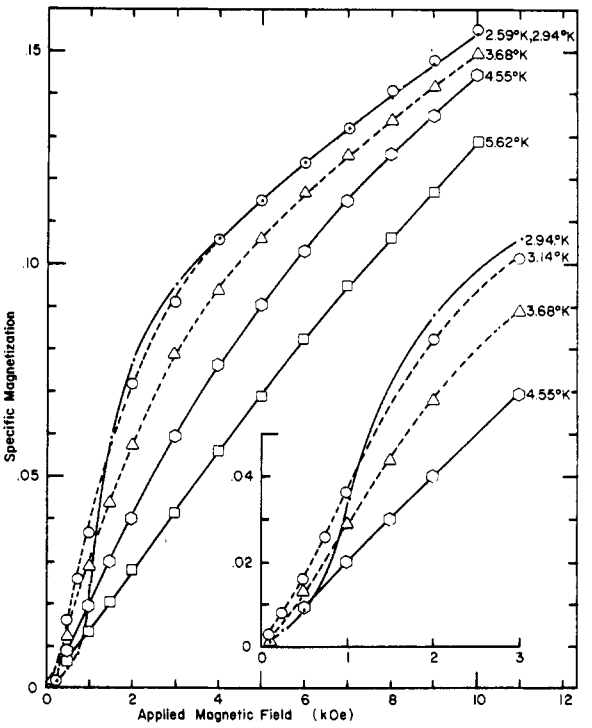

Figure 10. Specific magnetization vs. applied field strength for $Co(Hipp)_2(H_2O)_3 \cdot 2H_2O$ for temperatures below 6 K.

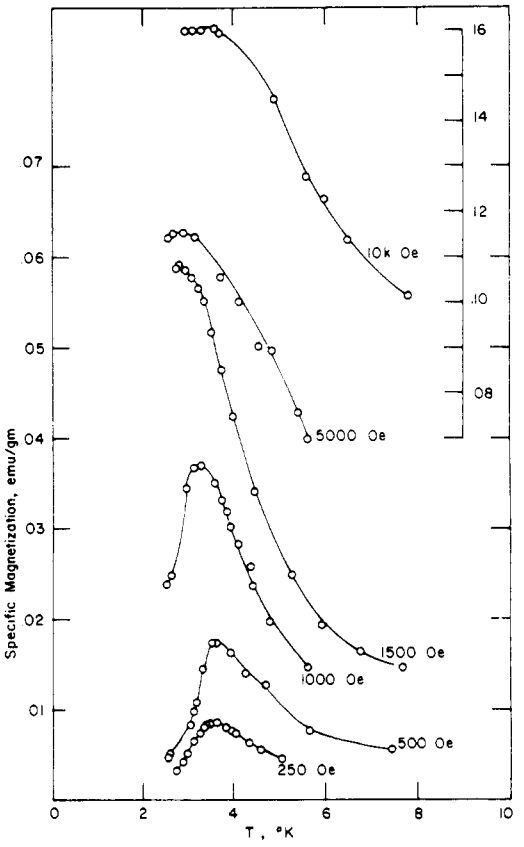

Figure 11. Specific magnetization vs. temperature for several values of applied magnetic field for $Co(Hipp)_2(H_2O)_3 \cdot 2H_2O$. Right-hand ordinate is for the curves at 10 kOe and 5000 Oe. Left-hand ordinate is for curves at 250, 500, 1000, and 1500 Oe.

r is any metal-metal distance. The shortest M-M* distance along the *a* axis is over 20 Å and is considered too large a distance for dipolar interactions to contribute to the ordering of

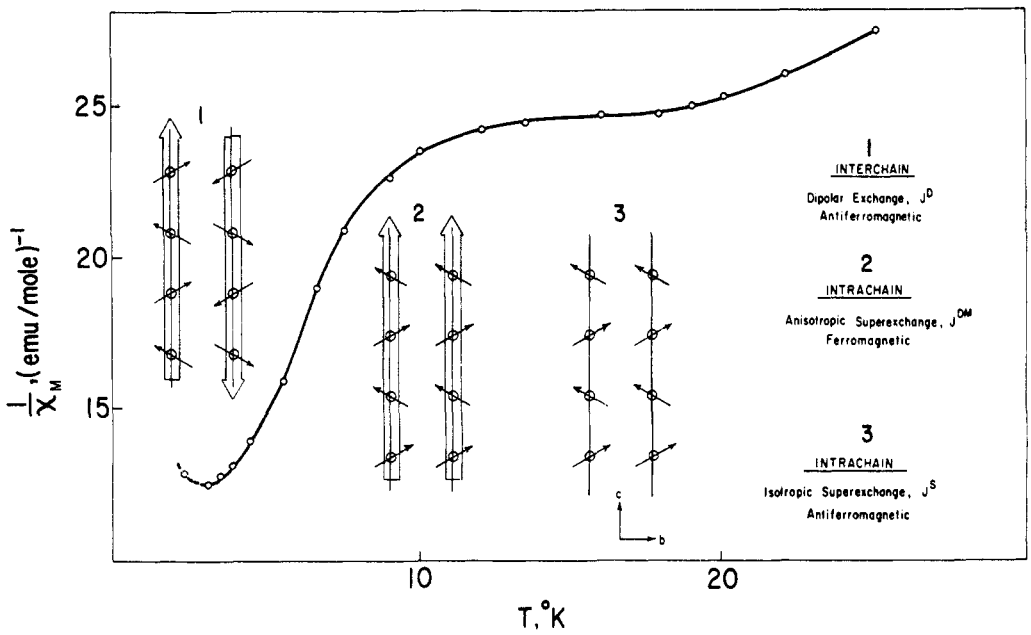

Figure 12. The proposed magnetic spin structure for the Ni(II) and Co(II) hippurates as illustrated by the $Co(Hipp)_2(H_2O)_3 \cdot 2H_2O$ magnetic susceptibility data. 1 is the ground state spin structure with chain moments alternating along the *b* axis. 2 and 3 arise from individual magnetic interactions being disrupted by adding kT energy to the system.

spins; in addition, the hippurate ligands extend out from the chain (see Figure 4) along this axis, further negating any interchain dipolar interactions. Dipolar interactions along the *b* axis ($r \sim 6.9$ Å for both compounds) are expected to be weak but evident above 1 K. Along the *c* axis (intrachain), $r \sim 3.9$ Å for both systems indicating that dipolar interactions should be strongest along this axis. If there is enough single ion anisotropy to induce dipolar coupling (see Introduction), then $|J_c^D| > |J_b^D| \gg |J_a^D| \simeq 0$, where J^D is the dipolar exchange energy.

Realizing that contributions to spin exchange are usually much greater from superexchange phenomena than through dipolar coupling, the above structural analyses predict $|J_c^S| > |J_c^D| > |J_b^D|$ and that all other interactions that have been considered do not contribute significantly above 1 K. Since neither superexchange nor dipolar exchange is possible along the *a* axis, it follows that magnetic ordering will occur in only one dimension (along the *c* axis) if the system consists of wholly isotropic metal ions. Since all magnetically concentrated compounds reported to date order in three dimensions (albeit some order only at temperatures below 1 K), the nickel and cobalt hippurates represent the first examples of a material expected to order in only two dimensions. To understand the nature of this unique ordering, the magnetization was studied as a function of the external field strength.

The field-dependent behavior of cobalt hippurate was examined in the region of increasing magnetic susceptibility (6–20 K); with fields of up to 12 kOe, the magnetization was observed to be independent of field strength (see Figure 9). If the phenomena occurring in this temperature range are ferromagnetic in origin, application of even a weak magnetic field would be expected to cause the spontaneous moment to follow the direction of the applied external field, exhibiting field-dependent behavior, i.e., a nonlinear response to the external field. To understand why the magnetization is not field dependent in this temperature range for cobalt hippurate, it is necessary to examine the field-dependent behavior of the antiferromagnetic transition which occurs below 6 K. This antiferromagnetic transition is shown to be field dependent in Figures 10 and 11. As these figures indicate, the magnetization isotherms obtained with fields up to 10 kOe in the temperature range of 2.6–6.6 K exhibit S-shaped curves below about 3.1 K. Furthermore, the specific magnetization maximum shifts to lower temperatures with increasing applied field strength and reaches an apparent saturation at about 5 kOe. This magnetic behavior is characteristic of a metamagnetic transition and is often observed to arise through dipole–dipole interactions.

The only known phenomena which appear to be compatible with the crystallographic data as well as the magnetic data arise through intrachain anisotropic superexchange. Although there is a pseudodipolar contribution, the largest contribution arises through the antisymmetric exchange of spin. This Dzyaloshimsky–Moriya (D–M) interaction is allowed only when the following conditions are met: (1) metal centers cannot be related to one another by a center of symmetry; and (2) there must be some single ion anisotropy ($J^{DM} \propto (g-2)/g$). When these conditions exist, the superexchange causes a net moment to be spontaneously built up perpendicular to the easy axis of magnetization. The nickel and cobalt hippurates have no center of symmetry between neighboring metal ions (a crystallographic result of canting metal octahedra) and possess a C_2 axis of symmetry parallel to the *b* axis passing through the bridging water molecule (see Figure 2). According to the symmetry rules worked out by Moriya for the antisymmetric exchange of spin, the spontaneous moment should be directed perpendicular to this C_2 axis.[17] Since the large majority of antiferromagnetic ordered chains have the easy axis perpendicular to the chain, this requires that the spontaneous moment be built up along the chain. Assuming this to be the case in the nickel and cobalt hippurates, the net spontaneous moment produced by the D–M interaction is expected to increase rapidly along the chain with decreasing temperature. As the temperature is lowered, the spontaneous moments on neighboring chains begin to effectively exchange through dipolar interactions. Since the magnetic moments are oriented "side on", the moments of alternating chains would be expected to reverse at some critical temperature ($T_c^b \simeq 3.1$ K, Co), resulting in a ground state which has an antiferromagnetically coupled configuration of net chain moments along the *b* axis. Realizing that an ordered antiferromagnet has no net spontaneous moment and that ordering of this antiferromagnetic ground state begins to occur above its critical temperature, it is not surprising that the magnetization of cobalt hippurate was

field independent at temperatures above T_c[b] where the susceptibility was observed to rapidly increase (6–15 K). The magnetic model for cobalt hippurate is summarized in Figure 12.

To understand the differences in the magnetic susceptibilities of cobalt and nickel hippurates, it is necessary to consider the mechanism of the D–M interaction. Herweijer et al.[15] derived the following expression for the magnitude of the D–M interaction as a function of the superexchange coupling constant, J^S, and the canting angle ϕ:

$$J^{DM} = -\frac{J^S \tan 2\phi}{2} \quad (6)$$

Since ϕ is nearly the same in the nickel and cobalt systems (21.4°, Ni; 25.9°, Co), the above expression reduces to

$$J^{DM} \approx -\frac{1}{2} J^S$$

As discussed earlier, J^S is a sensitive function of bond angles and bond distances; the crystallographic data as well as the magnetic susceptibility data indicate that $|J^S|$ should be largest for the nickel system. If the single ion anisotropy is assumed to be nearly equal for both ions, the above expressions predict $J^{DM}(Ni) > J^{DM}(Co)$. As can be seen from the magnetic susceptibility data (see Figures 6 and 7), the D–M interaction becomes evident at about 10–15 K in the cobalt system and at about 3 K in the nickel system, contradicting this prediction. This experimental evidence suggests that there must be large single ion differences between the nickel and cobalt ions since $J^{DM} \propto (g - 2)/g$.

An EPR spectrum of cobalt hippurate has not been observed at either room temperature or at 77 K; however, this is not unexpected since the cobalt(II) ion is notoriously anisotropic and is expected to give rise to a strong D–M interaction as observed. The nickel(II) ion is only slightly anisotropic (g = 2.2), indicating that the D–M interaction should be weak compared to the cobalt system. If the difference in single ion anisotropy is expected to be large as predicted here, then $J^{DM}(Co) > J^{DM}(Ni)$, as observed. Since the metamagnetic transition cannot begin to occur until the D–M interaction orders significantly (the closest M–M* = 6.9 Å), it is not surprising that the antiferromagnetic (metamagnetic) transition does not occur above 2.1 K in the nickel magnetic system. Since the D–M interaction is observable above 2.1 K, we expect that two-dimensional ordering will occur at a temperature >1 K in the nickel hippurate system.

In conclusion, it is interesting to note that similarities in the crystallographic structures predict basically the same possible phenomenon for both the nickel and cobalt hippurates: (1) intrachain isotropic superexchange (antiferromagnetic), (2) intrachain anisotropic superexchange (ferromagnetic), and (3) interchain dipolar metamagnetic exchange (antiferromagnetic). From this study, it appears that changes in structure between the nickel and cobalt systems have their greatest influence on determining the magnitude of isotropic exchange, and that, when anisotropic spin exchange is possible, the single ion anisotropy exhibits the greatest influence. One conclusion is that the effect of subtle differences in the crystallographic structure can be observed in the magnetic susceptibility only when ions of equal anisotropy are substituted into a particular crystallographic structure; conversely, if metal ions of different anisotropy are substituted, a corresponding change is expected in the anisotropic types of exchange.

Experiments are now underway to evaluate the magnetic properties of the nickel hippurate system below 2.2 K. Obviously, single-crystal magnetic susceptibility and neutron diffraction data are required for the absolute assignment of the spin structure. Owing to the nature of the nickel and cobalt hippurate crystals, efforts to grow a sample of the appropriate size for either of the above physical methods have been unsuccessful. Since there are no magnetic interactions between *bc* planes, perhaps the plate-like crystals thus far obtained may be stacked together to give a sample large enough for a single-crystal magnetic susceptibility determination. EPR experiments of both the nickel and cobalt systems are also being investigated at 4.2 K.

These studies indicate the utility of providing new series of molecular systems whose properties can be used to evaluate existing theoretical models. This series of α-amido acid complexes of the first-row transition metals promises to provide several new solid-state materials for modeling low-dimensional magnetic systems.

Acknowledgments. The authors would like to thank the National Science Foundation (Grant CHE 76-17434) for partial support of this research. Also partial support was supplied by the Warner-Lambert Pharmaceutical Co. The authors would also like to thank Dr. O. F. Griffith for his invaluable help with the EPR data.

References and Notes

(1) (a) University of New Orleans; (b) to whom correspondence should be addressed at the Division of Engineering Research, Louisiana State University, Baton Rouge, La. 70803; (c) E. I. du Pont de Nemours and Co.; (d) Southern University, New Orleans, La. 70126.
(2) (a) H. Eichelberger, R. Majeste, R. Surgi, L. Trefonas, M. L. Good, and D. Karraker, *J. Am. Chem. Soc.*, **99**, 616 (1977); (b) M. L. Good, H. R. Eichelberger, R. Seidler, E. Schaeffer, G. L. McPherson, and D. Karracker, *Inorg. Chem.*, to be submitted.
(3) R. L. Carlin and A. J. van Duyneveldt, "Magnetic Properties of Transition Metal Compounds", Springer-Verlag, New York, 1977.
(4) E. Ising, *Z. Phys.*, **31**, 253 (1925).
(5) L. J. de Jongh and A. R. Miedema, *Adv. Phys.*, **23**, 1 (1974), and references cited therein.
(6) F. A. Cotton, *Acc. Chem. Res.*, **11**, 225 (1978).
(7) B. Bleaney and K. D. Bowers, *Proc. R. Soc. London, Ser. A*, **214**, 451 (1952).
(8) G. M. Brown and R. Chidambaram, *Acta Crystallogr., Sect. B*, **29**, 2393 (1973).
(9) W. E. Hatfield, "Extended Interactions between Metal Ions", Vol. 10, L. V. Interrante, Ed., ACS Symposium Series, American Chemical Society, Washington, D.C., 1974, p 108.
(10) D. J. Hodgson, *Prog. Inorg. Chem.*, **19**, 173 (1975).
(11) R. P. Scaringo, R. Singh, R. P. Eckberg, W. E. Hatfield, and D. J. Hodgson, *Inorg. Chem.*, **14**, 1127 (1975).
(12) J. T. Veal, W. E. Hatfield, D. V. Jetter, J. C. Hempel, and D. J. Hodgson, *Inorg. Chem.*, **12**, 342 (1973).
(13) (a) E. A. Boudreaux and L. M. Mulay, Eds., "Theory and Applications of Molecular Paramagnetism", Wiley, New York, 1976, Chapter 7. (b) NOTE ADDED IN PROOF: It should be pointed out that Anderson has theoretically developed a general model which predicts the ferromagnetic (90°) and antiferromagnetic (180°) interactions on the basis of orbital overlap involved in the superexchanged pathway. Much of the early experimental evidence for Anderson's theory involves the Cu(II) and Cr(III) systems, since the structures and magnetic properties for many of these compounds were already known [P. W. Anderson, *Magnetism*, **1**, 25 (1963); *Solid State Phys.*, **14**, 99 (1963)].
(14) N. Thorups and J. Soling, *Acta Chem. Scand.*, **23**, 2933 (1969).
(15) A. Herweijer, W. J. M. de Jonge, A. C. Botterman, A. L. M. Bongaarts, and J. A. Cowen, *Phys. Rev. B*, **5**, 4618 (1972).
(16) I. Dzyaloshinsky, *J. Phys. Chem. Solids*, **4**, 241 (1958).
(17) T. Moriya, "Magnetism", Vol. 1, G. T. Rodo and H. Suhl, Eds., Academic Press, New York, 1963, Chapter 3.
(18) E. Stryjewski and N. Giordano, *Adv. Phys.*, **26**, 487 (1977).
(19) L. Berger and S. A. Friedberg, *Phys. Rev. A*, **136**, 158 (1964).
(20) H. R. Eichelberger, Ph.D. Dissertation, University of New Orleans, 1975.
(21) J. N. Brown and L. M. Trefonas, *Org. Prep. Proced.*, **2**, 317 (1970).
(22) G. Marcotrigiano and G. C. Pellacani, *Inorg. Nucl. Chem. Lett.*, **11**, 643 (1975).
(23) The conventional reliability index $R = \Sigma w||kF_o| - |F_c||/\Sigma wkF_o|$ is cited. Scattering factors for carbon, nitrogen, oxygen, and cobalt are taken from the paper by D. Cromer and J. Waber, *Acta Crystallogr.*, **18**, 104 (1965), while that for hydrogen is from "International Tables for X-ray Crystallography", Vol. III, Kynoch Press, Birmingham, England, 1968.
(24) J. N. Brown, H. R. Eichelberger, E. Schaeffer, M. L. Good, and L. M. Trefonas, *J. Am. Chem. Soc.*, **93**, 6290 (1971).
(25) J. N. Brown and L. M. Trefonas, *Inorg. Chem.*, **12**, 1730 (1973).
(26) J. Ferguson, *J. Chem. Phys.*, **32**, 533 (1960).
(27) M. E. Fisher, *Am. J. Phys.*, **32**, 343 (1964).